PASJ: Publ. Astron. Soc. Japan , 1–**??**,

What Kinds of Accretion Disks Are There in the Nuclei of Radio Galaxies?

Osamu KABURAKI,* Takanobu NANKOU, Naoya TAMURA, and Kiyoaki WAJIMA
Domain for Fundamental Sciences, Graduate School of Science and Engineering,
Yamaguchi University, Yamaguchi 753–8512
okab@amail.plala.or.jp, wajima@yamaguchi-u.ac.jp

(Received ; accepted)

Abstract

It seems to be a widely accepted opinion that the types of accretion disks (or flows) generally realized in the nuclei of radio galaxies and in further lower mass-accretion rate nuclei are inner, hot, optically thin, radiatively inefficient accretion flows (RIAFs) surrounded by outer, cool, optically thick, standard type accretion disks. However, observational evidence for the existence of such outer cool disks in these nuclei is rather poor. Instead, recent observations sometimes suggest the existence of inner cool disks of non-standard type, which develop in the region very close to their central black holes. Taking NGC 4261 as a typical example of such light eating nuclei, for which both flux data ranging from radio to X-ray and data for the counterjet occultation are available, we examine the plausibility of such a picture for the accretion states as mentioned above, based on model predictions. It is shown that the explanation of the gap seen in the counterjet emission in terms of the free-free absorption by an outer standard disk is unrealistic, and moreover, the existence itself of such an outer standard disk seems very implausible. Instead, the model of RIAF in an ordered magnetic field (so called resistive RIAF model) can well serve to explain the emission gap in terms of the synchrotron absorption, as well as to reproduce the observed features of the overall spectral energy distribution (SED). This model also predicts that the RIAF state starts directly from an interstellar hot gas phase at around the Bondi radius and terminates at the inner edge whose radius is about 100 times the Schwartzschild radii. Therefore, there is a good possibility for a cool disk to develop within this innermost region.

Key words: galaxies: accretion, accretion disks — galaxies: jets — galaxies: individual (NGC 4261) — magnetic field

1. Introduction

Now, it has become a great paradigm in astrophysics that accretion flows onto compact objects drives various types of activities, such as those seen in the active galactic nuclei (AGNs) and their associated jets, γ-ray bursters, bursts and jets in Galactic X-ray binaries and so on. However, the state of affairs is still far from settled as for the detailed specifications of the nature (or kind) of related accretion disks (or flows) in these various circumstances.

It is commonly accepted that the most essential parameter to control the states of accretion flows is the dimension-less mass accretion rate, $\dot{m}$, normalized to the Eddington rate of a central object (Frank et al. 2002; Armitage 2004; Kato et al. 2008). When $\dot{m} \sim 1$, geometrically thin, radiatively efficient so-called standard disks (Shakura & Sunyaev 1973) would develop, and when $\dot{m}$ further exceeds a certain limit, optically thick but radiatively inefficient accretion flows (often called slim disks) appear. Therefore, both these states are expected to be realized in luminous AGNs such as quasars and Seyfert galaxies whose accretion rates are believed to be large and amount to a considerable fractions of the Eddington limit.

On the other hand, when the accretion rate is very small in the sense that $\dot{m} \ll 1$, the flows become optically thin and radiatively inefficient. Usually, only this specific branch is called the radiatively inefficient accretion flows (RIAFs). RIAFs are, therefore, expected to appear in the low luminosity AGNs (LLAGNs) such as the nuclei of low-excitation radio galaxies (LERGs, see e.g., Evans et al. 2007) and of most nearby galaxies (Ho 2008), at least in the inner parts of their accretion regions (e.g., Narayan 2002).

The explicit doubts for the presence of pure standard disks in luminous AGNs have been cast, e.g., by Leahy (1999) and Gaskell (2008). Leahy insists that the origin of the big blue bump (BBB) needs reconsideration because i) the lack of strong EUV lines suggests the emission not caused by bremsstrahlung, ii) the accretion disk cannot be a simple standard one since the observed spectra extend to X-rays and iii) the disk should be much smaller than that conceived in the standard model, as the tight correlation within 1 hour of the variations in UV and optical bands suggests. The doubt of Gaskell is mainly based on the facts that i) the overall shapes of the spectral energy distribution (SED) of AGNs are nearly flat excluding BBB in the sense that $\nu F_\nu \sim$ const., where ν and F_ν are the frequency and associated flux, respectively, and ii) the frequency dependence of F_ν in BBB largely deviates from the prediction of the standard disk model, $F_\nu \propto \nu^{1/3}$.

For LLAGNs, the absence of the standard disk, at least in its original form, has been suspected observationally. It is reported (e.g., Chiaberge et al. 1999; Chiaberge et al. 2000) that in most of the FR I samples examined by *Hubble Space Telescope* (*HST*) there exist unresolved optical sources ($\lesssim 0.01$ pc), named central compact cores (CCCs), which show good correlation with the flux of radio cores. However, the evidence

* Present address: Otomaru-machi 249, Hakusan-shi, Ishikawa 924-0826

for the presence of standard disks is not detected, and the disks are supposed to be of RIAF type.

Recently, Maoz (2007) argues that in SED of most LLAGNs ($\sim 10^{40}$ erg s^{-1}) the contribution from UV is not weak and is similar to those of Seyfert 1 ($\sim 10^{44}$ erg s^{-1}), though the radio/UV ratio increases according to the decreasing luminosity of LLAGNs. This means that the emission ranging from UV to X-ray is rather insensitive to AGN luminosity, whereas the radio luminosity increases as AGN luminosity decreases. He insists, therefore, that there exist some type of cool thermal disks with low accretion rates in the inner parts of most nearby LLAGNs. The existence of inner cool disks in LLAGNs has also been put forward based on the analogy between the low/hard state of Galactic X-ray binaries and the state in jet-dominated LLAGNs (e.g., Livio et al. 2003). In the case of X-ray binaries, many observational evidences for the presence of inner cool disks are now accumulating (e.g., Miller et al. 2006; Rykoff et al. 2007).

For the class of AGNs in which the mass accretion rates are believed to be larger than in LLAGNs, the presence of the inner cool disks is suggested by observations even more strongly. For example, in broad-line radio galaxies (BLRGs), which are classified as type 1 AGNs (see, e.g., Urry & Padovani 1995) and belong to the class of high-excitation radio galaxies (HERGs, see e.g., Evans et al. 2007) that have larger accretion rates than LERGs, the existence of untruncated cool, thermal disks almost down to the inner-most stable circular orbit (ISCO) is insisted (e.g., Ballantyne et al. 2002; Ballantyne & Fabian 2005). Their spectral fittings further suggest that the cool disks do not need to extend beyond several or tens of the Schwarzschild radii. For Seyfert galaxies, the presence of a compact cool disk around each central black hole has been established more firmly from X-ray spectra obtained by *XMM-Newton* (e.g., Nandra et al. 2006).

It is interesting to see that the importance of inner cool disks has begun to draw much attention also from theoretical side. In fact, the presence of such geometrically-thin, optically-thick accretion disks in the innermost regions of accretion flows have been proposed for a long time (e.g., Pringle et al. 1973; Rees et al. 1982; Begelman et al. 1987; Haardt & Maraschi 1991; Svensson & Zdziarski 1994; Fabian & Rees 1995; Merloni & Fabian 2002; Livio et al. 2003; Kuncic & Bicknell 2004; 2007). Among them, Kuncic & Bicknell (2007) clearly demonstrate the role played by the vertical component of a global magnetic field in extracting energy and angular momentum from the accretion disk and in dissipating energy in the corona sandwiching the disk. Such a disk-corona structure developed very close to the central black hole is now believed to be the most plausible site of jet launching.

It is often argued that a RIAF develops only within the truncation radius r_t, which forms the inner edge of a standard disk extending outside (Esin et al. 1997; Narayan et al 1998; Cao 2004; Yuan 2007). Observationally, however, the nucleus of our Galaxy (Sgr A*) has been marginally resoled by *Chandra* X-ray Observatory revealing that the hot accretion flow starts roughly from its Bondi radius (Baganoff et al. 2003, see also the spectral fittings by Yamazaki et al. 2002). Also, there is a proposition based on observations of radio-loud AGNs that there are two phases for their accretion flows, in which

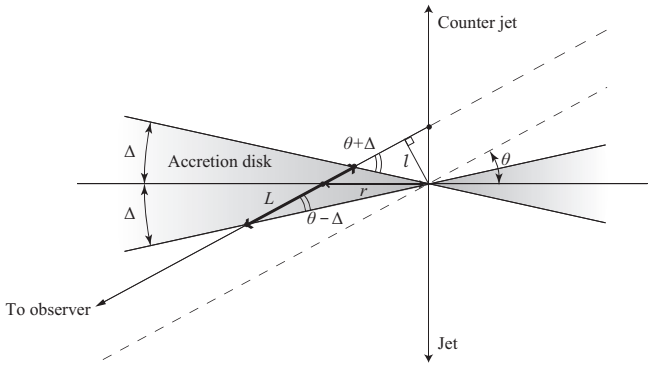

Fig. 1. An illustration of the geometrical configuration considered in the text. The polar axis indicates the direction of jet and counterjet. Suspected presence of an inner cool disk is neglected here.

LERGs accrete hot surrounding gas directly from their Bondi radii whereas HERGs accrete cold dense gas (Best et al. 2005, Hardcastle et al. 2007, Evans et al. 2007).

Standing in such a new trend as reviewed above, we concentrate in this paper especially on the problem, if or not a standard-type accretion disk can exist in the outer region of an accretion flow of radio galaxies and LLAGNs. As a typical example of such low accretion-rate nuclei, we discuss the case of NGC 4261. However, we expect that the results obtained here would apply generally to the galaxies of similar type. The main clue to solve our problem is the occultation of counterjet by its associated accretion disk.

In §2, the observational facts related to the emission gap in the counterjet of NGC 4261 are described briefly. The implausibility of interpreting this gap by the free-free absorption of a radiatively-cooled accretion disk of conceivable types is discussed in §3, and the plausibility of interpreting it as the synchrotron absorption of a RIAF in a global magnetic field is roughly shown in §4. The reliability of the latter interpretation is further confirmed in §5 by performing numerical calculations based on our own RIAF model, in the course of global spectral fittings. The final section summarizes the results obtained.

2. Counterjet Absorption in NGC 4261

NGC 4261 is an FR I radio galaxy located at 30 Mpc from our Galaxy and the mass of its central black hole is estimated to be $(5 \pm 1) \times 10^8 M_\odot$ (Ferrarese et al. 1996). As discussed in detail in Jones et al. (2000; 2001), the emission from bipolar radio jets shows a narrow gap on the east side of the central core, which is regarded as the counterjet. They have pointed out that this gap can be interpreted as an absorption caused by the accretion disk surrounding the central black hole.

Here, we quote from their papers the values of the geometrical parameters (see Fig. 1) that are necessary for the following discussion. The angle between the equatorial plane (assumed to be normal to the jet axis) and a line of sight is $\theta = 26°$. The half-opening angle of the geometrically thin accretion disk, $\Delta = \phi/2 = 6.5°$ (full-opening angle is ϕ according to their notation), is inferred from the HI observations of van Langevelde et al. (2000). Therefore, the projected distance from the center to the line of sight,

$$l = r\sin\theta = r^*\sin(\theta - \Delta), \quad (1)$$

becomes $l = 0.44\,r$, where r is the equatorial distance and r^* is the surface distance from the center, respectively. Further, the path length through the disk,

$$L = l\{\cot(\theta - \Delta) - \cot(\theta + \Delta)\}, \quad (\theta \geq \Delta > 0) \quad (2)$$

is $L = 1.3\,l$.

Combining these results, we have $L(x) = 0.57 x r_{\rm S}$ for the line of sight which crosses the equatorial plane at a given radius r, where $x \equiv r/r_{\rm S}$ is the non-dimensional radius normalized to the Schwarzschild radius, $r_{\rm S} = 2GM/c^2$, of the central black hole of mass M. Jones et al. (2001) have derived from their observation at 8.4 GHz that $l = 0.23$ pc for the projected distance from the core to the center of the coujerjet absorption. This value corresponds to $r = 0.52$ [pc] ($x = 1.0 \times 10^4$) and $L = 0.3$ [pc], respectively.

When the absorption coefficient $\alpha_\nu(x)$ at a given frequency ν is given on the equatorial plane as a function radius r, we estimate the optical thickness across the disk along the line of sight roughly as

$$\tau_\nu(x) = \frac{1}{2}\alpha_\nu(x) L(x). \quad (3)$$

3. Free-free Absorption by Radiatively Cooled Disks

Although Jones et al. (2000; 2001) discussed the possibility of interpreting the gap in the counterjet as due to the free-free absorption by an optically thin accretion disk developed in its nuclear region, it does not seem to be plausible. This is because they fix the temperature in the disk arbitrarily at $\sim 10^4$ K and hence the consistency of their model is not guaranteed. In fact, if the disk is optically thin and hence radiatively inefficient, the gas temperature is expected to rise close to the virial one. Then, the dominant cooling mechanism is not the free-free emission but would be the inverse Compton cooling. The self-consistent model for such a situation is known as SLE model (Shapiro et al. 1976; Kato et al. 2008), which is however thermally unstable. Thus, the absorption of counterjet emission by a radiation-cooled, optically-thin disk is anyway implausible.

Therefore, we examine next the possibility that the absorption is due to a radiatively-efficient, optically-thick disk of the standard type. According to the results of Shakura & Sunyaev (1973), we cite the expressions for relevant physical quantities in the standard accretion disk. They are expressed as functions of the normalized radius x and subsidiary three parameters. The parameters are all non-dimensional quantities. They are the viscosity parameter α, the mass of a central black hole $m \equiv M/10^8 M_\odot$, and the mass accretion rate $\dot{m} \equiv \dot{M}/\dot{M}_{\rm Edd}$ in the disk, where $M_{\rm Edd} = L_{\rm Edd}/c^2$ is the Eddington accretion rate. Note that the normalizations adopted here for x, m and $\dot{m}$ are different in part from both of those adopted in Frank et al. (2002) and Kato et al. (2008).

Generally, the standard disk is divided into three regions according to the physical conditions realized in it. The opacity is dominated by the electron scattering in the inner and middle regions, whereas the free-free opacity dominates in the outer region. The radiation pressure dominates over the gas pressure in the inner region, and *vice versa* in the middle and outer regions.

The temperature, gas density and disk half-thickness in each region are as follows.

(I) Inner region:

$$T = 3.7 \times 10^5 \alpha^{-1/4} m^{-1/4} x^{-3/8}\ [{\rm K}], \quad (4)$$

$$\rho = 6.0\ \alpha^{-1} m^{-1} \dot{m}^{-2} x^{3/2}\ [{\rm g/cm^3}], \quad (5)$$

$$H = 2.3 \times 10^{13} m\dot{m}\ [{\rm cm}]. \quad (6)$$

(II) Middle region:

$$T = 8.1 \times 10^6 \alpha^{-1/5} m^{-1/5} \dot{m}^{2/5} x^{-9/10}\ [{\rm K}], \quad (7)$$

$$\rho = 2.1 \times 10^{-5} \alpha^{-7/10} m^{-7/10} \dot{m}^{2/5} x^{-33/20}\ [{\rm g/cm^3}], \quad (8)$$

$$H = 1.9 \times 10^8 \alpha^{-1/10} m^{9/10} \dot{m}^{1/5} x^{21/20}\ [{\rm cm}]. \quad (9)$$

(III) Outer region:

$$T = 1.0 \times 10^6 \alpha^{-1/5} m^{-1/5} \dot{m}^{3/10} x^{-3/4}\ [{\rm K}], \quad (10)$$

$$\rho = 1.0 \times 10^{-4} \alpha^{-7/10} m^{-7/10} \dot{m}^{11/20} x^{-15/8}\ [{\rm g/cm^3}], \quad (11)$$

$$H = 3.3 \times 10^{10} \alpha^{-1/10} m^{9/10} \dot{m}^{3/20} x^{9/8}\ [{\rm cm}], \quad (12)$$

$$\tau_{\rm R} = 2.2 \times 10^3 \alpha^{-4/5} m^{1/5} \dot{m}^{1/5}. \quad (13)$$

The final quantity $\tau_{\rm R}$ represents the Rosseland-mean free-free optical depth vertically across the disk, i.e., $\tau_{\rm R} \equiv \alpha_{\rm R} H$, which is determined self-consistently within the standard model.

The radii of the boundaries between the regions I∼II and II∼III are given by

$$x_1 = 3.5 \times 10^2\ \alpha^{2/21} m^{2/21} \dot{m}^{16/21}, \quad (14)$$

$$x_2 = 1.1 \times 10^3 \dot{m}^{2/3}, \quad (15)$$

respectively.

Based on the above equations, we discuss the physical conditions expected to appear in the putative standard disk in the nucleus of NGC 4261. The viscosity parameter is usually assumed to be in the range $\alpha = 0.01 \sim 0.1$, and is tentatively fixed as $\alpha = 0.1$ here. Other parameters are fixed at $m \sim 5$ and $\dot{m} \sim 10^{-3}$. The former value has been mentioned in the previous section, and the latter is set at the reference value adopted in Jones et al. (2000). These values yield for the radii of the boundaries, $x_1 = 1.5$ and $x_2 = 11$. This means that the major part of the accretion disk is in the state called the outer region, except for the innermost part ($x \lesssim 10$) where the standard model itself could be inaccurate owing to general relativistic effects.

Since the occultation by the accretion disk is expected to occur at $x \gtrsim 10^3$ (Jones et al. 2000; 2001), only the outer region is of our interest here, in which the quantities vary like

$$T = 1.5 \times 10^5 x^{-3/4}\ [{\rm K}], \quad (16)$$

$$\rho = 3.6 \times 10^{-5} x^{-15/8}\ [{\rm g/cm^3}], \quad (17)$$

$$n_e = 2.2 \times 10^{18} x^{-15/8}\ [{\rm cm^{-3}}], \quad (18)$$

where the electron number density n_e is calculated by assuming full ionization for a purely hydrogen gas. At a location of $x = 10^3$, for example, we have $T = 8.2 \times 10^2$ [K], $\rho = 8.6 \times 10^{-12}$ [g/cm^3], $n_e = 5.2 \times 10^{12}$ [cm^{-3}] and for the

Rosseland-mean optical depth, $\tau_{\rm R} = 4.8 \times 10^3$, which becomes independent of the radius in this region.

More specifically, the frequency dependent free-free absorption coefficient is written (Rybicki & Lightman 1979) as

$$\alpha_\nu^{\rm ff} = 1.8 \times 10^{-2} T^{-3/2} n_e^2 \nu^{-2} \bar{g}_{\rm ff} \ [{\rm cm}^{-1}], \tag{19}$$

where $\bar{g}_{\rm ff}$ is the velocity averaged Gaunt factor and we put $\bar{g}_{\rm ff} = 1$ below for simplicity. The optical depth for the free-free absorption at 8.4 GHz calculated from equations (19) and (3) is extremely large at any reasonable radius in the outer region, $x > x_2 \simeq 10$.

Thus, the standard disk cannot provide a preferable value, $\tau \sim 1$ (Jones et al. 2001), to reproduce the emission gap of the counterjet. Moreover, the resulting temperature is too low to maintain a sufficient degree of ionization in the region $x \gtrsim 10^2$, which is necessary for the free-free processes to be important. In conclusion, the interpretation of the gap observed in the counterjet emission from NGC 4261 by the free-free absorption due to a standard-type accretion disk is very implausible. Moreover, since such a low temperature obtained above contradicts to the basic assumptions of the standard disks, it casts strong doubt even on the existence of a standard disk in the accretion flow of this object, and also of a similar type radio galaxy, at least, on the outside of the RIAF regions.

In a similar case of NGC 6251, Sudou et al. (2000) have already pointed out such difficulties as appeared above in interpreting the emission gap in terms of the free-free absorption by a radiation cooled disk of any type. Also for similar reasons, Liu et al. (2003) have presented an alternative interpretation of this phenomenon.

4. Synchrotron Absorption by Resistive RIAF

In the recent decade, a model of RIAF in a global magnetic field has proved its plausibility and applicability to LLAGNs (Kaburaki 2000; 2001; 2007; Kino et al. 2000; Yamazaki et al. 2002). Also, the direct connection of this type of accretion disks to FR I jets have been strongly suggested (Kaburaki 2009). Hereafter we call it the 'resistive' RIAF model, in order to distinguish it from the well known 'viscous' RIAF model in which the presence of a global magnetic field is neglected (see, e.g., Narayan et al 1998). In the former model, the resistive heating (probably of anomalous type) due to the electric current caused in an accretion disk plays a dominant role to dissipate the gravitational energy, instead of the viscous heating in the latter model. Although some type of turbulent magnetic fields are assumed to present in a disk also in the viscous RIAF model, it is a great advantage of the resistive RIAF model that this can specify the strength of the ordered magnetic field self-consistently within the model. In this section, we therefore try to interpret the counterjet absorptions in NGC 4261 within the framework of the resistive RIAF model.

The relevant quantities are given (Kaburaki 2001, Yamazaki et al. 2002) in this model as

$$T = 9.0 \times 10^{11} x^{-1} \ [{\rm K}], \tag{20}$$

$$n_e = 9.0 \times 10^{10} (2n+1)^{-1/2} \Re_0^{\ 2(n+1)} x_{\rm out}^{\ -(1/2+2n)} \times m^{-1} \dot{m} x^{-(1-2n)} \ [{\rm cm}^{-3}], \tag{21}$$

$$|b_\varphi| = 2.4 \times 10^4 (2n+1)^{-1/4} \Re_0^{\ n+1} x_{\rm out}^{\ -(1/4+n)} \times m^{-1/2} \dot{m}^{1/2} x^{-(1-n)} \ [{\rm G}], \tag{22}$$

where b_φ denotes the azimuthal component of the magnetic field.

Five non-dimensional parameters appeared above are as follows. The normalized mass, m, and the mass accretion rate, $\dot{m}$, are the same as before. However, since the model generally allow for the presence of a wind from the disk surfaces whose strength is specified by the wind parameter n ($-1/4 < n < 1/2$, where negative n corresponds to a down flow), the accretion rate becomes a function of radius. The parameter $\dot{m}$ here refers to its value at the outer edge of an accretion disk, $x_{\rm out} \equiv r_{\rm out}/r_{\rm S}$. In the resistive RIAF model, the radius of the outer edge $r_{\rm out}$ is identified as the Alfvén radius (which is of the same orders of magnitude as the Bondi radius, see Kaburaki 2007) whose value is a function of the surrounding gas temperature, and hence it is treated also as a parameter. The final parameter $\Re_0$ denotes the magnetic Reynolds number of the accretion flow, at the outer edge (the finiteness of this number corresponds to the name, 'resistive' MHD).

The resistive RIAF is geometrically thin in spite of its virial-like high temperature. This is because the magnetic pressure due to the azimuthal component, which is developed outside the disk by the disk rotation, compresses the plasma into a thin disk geometry (see Fig.2 of Kaburaki 2007). The half-opening angle of the disk is determined in terms of $\Re_0$ as $\Delta = \Re_0^{-(2n+1)}$. The inner edge radius is also specified in the model from the magnetic flux conservation as $x_{\rm in} = \Re_0^{-2} x_{\rm out}$. In the innermost region within this radius (i.e., $x < x_{\rm in}$), the basic assumptions used to derive the model becomes invalid. Although this region locates on the outside of the applicability of this model, this model anticipates in this manner the appearance of an essentially different accretion state in this innermost region.

Here, we briefly discuss the synchrotron processes within the framework of the resistive RIAF model. Since the temperature in the disk ($x_{\rm in} < x < x_{\rm out}$ with $x_{\rm in} \simeq 10^2$ and $x_{\rm out} \simeq 10^4$) is in the range $10^8 \lesssim T \lesssim 10^{10}$, the electron temperature can be regarded as mildly relativistic. In this case, the synchrotron emissivity averaged over the relativistic Maxwellian distribution becomes (Mahadevan et al. 1996)

$$j_\nu d\nu = \frac{\sqrt{2} e^2 n_e \omega_{\rm L}}{3c} \frac{\chi}{K_2(1/\theta_e)} \exp\left\{-1.89\, x_{\rm M}^{1/3}\right\} d\nu, \tag{23}$$

where e is the charge unit, m_e is the electron mass, $\omega_{\rm L} \equiv eB/m_e c$ is the Larmor frequency, and K_2 denotes the modified Bessel function of order 2. Other notations are $\chi \equiv \omega/\omega_{\rm L}$, $\theta_e \equiv k_{\rm B} T/m_e c^2$, and $x_{\rm M} \equiv 2\chi/3\theta_e^2$. Assuming a local thermodynamic equilibrium (LTE) in the accretion disk, we have for the synchrotron absorption coefficient in the Rayleigh-Jeans limit

$$\alpha_\nu^{\rm sy} = \frac{\sqrt{2}\pi e^2 c}{3 k_{\rm B}} \frac{n_e}{\nu T} \frac{\exp\left\{-1.89\, x_{\rm M}^{1/3}\right\}}{K_2(1/\theta_e)}. \tag{24}$$

For the discussion of NGC 4261, we set $n = 0$ (i.e., the wind is neglected) for simplicity and $\Re_0 \simeq 10$. The latter value yields the result $\Delta \simeq 0.1 = 5.7°$, which is consistent with the obser-

vation ($\phi/2 = 6.5^\circ$). Further, when we adopt the outer edge radius of $x_{\rm out} \simeq 10^4$ and $\dot{m} = 10^{-2}$ (this value is 10 times larger than that adopted by Jones et al. 2000) as suggested by our spectral fittings (see, figure 2), we obtain for the inner edge radius, $x_{\rm in} \simeq 10^2$, and for the physical quantities in the disk,

$$T = 9.0 \times 10^{11} x^{-1}\ [\mathrm{K}], \tag{25}$$

$$n_e = 1.8 \times 10^{7} x^{-1}\ [\mathrm{cm}^{-3}], \tag{26}$$

$$|b_\varphi| = 3.4 \times 10^{2} x^{-1}\ [\mathrm{G}]. \tag{27}$$

The final quantity, $|b_\varphi|$, should be substituted for B in the above synchrotron formulae.

Based on this model, we first confirm that the free-free opacity is negligible in the resistive IRAF applied to NGC 4261. Substituting $\nu = 8.4 \times 10^9$ [Hz] and the expressions for T and n_e, we obtain

$$\alpha^{\rm ff}_{8.4} = 9.7 \times 10^{-24} x^{-1/2}, \quad \tau^{\rm ff}_{8.4} = 4.1 \times 10^{-10} x^{1/2}. \tag{28}$$

The free-free optical depth is indeed negligibly small even at $x = 10^4$.

For the observational frequency of $\nu = 8.4 \times 10^9$ [Hz], the parameters related to the synchrotron process are calculated as $1/\theta_e = 6.6 \times 10^{-3}\, x$, $\chi\theta_e = 4.3 \times 10^2$, and $x_{\rm M}^{1/3} = 4.3 \times 10^{-2}\, x$. Therefore, roughly speaking, $1/\theta_e \gg 1$ except in the region very close to the inner edge where $1/\theta_e \sim 1$. In order to estimate the importance of the synchrotron absorption, we therefore use the asymptotic form of the modified Bessel function $K_2(z) \sim \sqrt{\pi/2z}\ e^{-z}$ in the limit of $z \to \infty$. In the region close to the inner boundary, however, the accuracy may be not so good.

Then, the approximate form of the synchrotron absorption coefficient becomes

$$\alpha^{\rm sy}_\nu \simeq \frac{2\sqrt{\pi} e^2 c}{3 k_{\rm B}} \frac{n_e}{\nu T \theta_e^{1/2}} \exp\left\{1/\theta_e - 1.89\, x_{\rm M}^{1/3}\right\}. \tag{29}$$

The existence of the exponential factor in the above formula implies that the importance of absorption rapidly decrease in the outer regions of the resistive RIAF where x is very large. Combining this expression with equation (3), we can calculate the position x at which $\tau^{\rm sy}_{8.4} \sim 1$ is realized. The result in our case gives $x = 322$. Although this value seems to be somewhat smaller than the observational value of $x \simeq 10^3$ (Jones et al. 2000), we cannot say too much because the above treatment is too crude, especially, near the disk's inner boundary ($x_{\rm in} \sim 100$, see the next section) which is close to the estimated radius of $\tau^{\rm sy}_{8.4} \sim 1$.

Nevertheless, we can say from the above discussion that the resistive RIAF model predicts the existence of rather narrow region near the disk's inner edge, in which the synchrotron absorption becomes appreciable. Therefore, this region can contribute to the formation of such a narrow gap as observed in the counterjet emission from NGC 4261 (and also from similar objects). This point will be further discussed in the next section in relation to detailed numerical calculations of the emission spectrum. Within the inner edge radius, the accretion flow is expected to form a condensed cool disk owing to efficient synchrotron cooling. Such an inner disk might also contribute to the absorption of counterjet emission. However, detailed discussions have to await the appearance of a concrete inner disk model.

5. Radiative Processes in Resistive RIAF

Although a crude estimation of synchrotron processes has indicated in the previous section a very good possibility of interpreting the gap seen in the counterjet emission of NGC 4261 as synchrotron absorption by a foreground resistive RIAF disk, further detailed confirmation of this possibility is given in this section based on numerical treatments of the relevant processes within the framework of the resistive RIAF model.

5.1. Reproduction of global SED

In this subsection, we want to prove persuasive abilities of the resistive RIAF model by reproducing the observational wide range SED. In figure 2, we plot luminosity νL_ν against frequency ν. Each curve there represents only the radiation from an accretion disk of the RIAF type which extends from the outer edge radius, $r_{\rm out} = x_{\rm out} r_{\rm S}$ (roughly corresponds to the Bondi radius), down to the inner edge radius, $r_{\rm in} = x_{\rm in} r_{\rm S}$. In actual situations, however, there may be other contributions, e.g., from bipolar jets and from an inner cool disk. The observational data are adopted from Ho (1999) and Balmaverde et al. (2006). Since the radiation in the radio wave band is very likely to come mainly from the jet component, we try to fit our calculated curves to the data points in the two frequency ranges, that from near-infrared (NIR) to infrared (IR) and that in X-rays.

The resistive RIAF model has 5 parameters to specify. They are mass of the central black hole m, outer edge radius of the disk $x_{\rm out}$, mass accretion rate (at the outer edge) $\dot{m}$, magnetic Reynolds number (at the outer edge) $\Re_0$, and wind parameter n. As already described, we can roughly fix two parameters as $m = 5$ and $\Re_0 = 10$ (or $\Delta = \phi/2 \simeq 0.1 = 5.7^\circ$) based on observations. The values of the remaining parameters are varied and are cited in figure 2 for each curve shown there. As seen from these curves, the disk radiation consists mainly of three peaks in different frequency ranges. They are labeled as S, B, and C for convenience, whose emission mechanisms are attributed, respectively, to thermal synchrotron emission, thermal bremsstrahlung, and their inverse Compton scatterings.

The method for calculating these contributions are given in Kino et al. (2000), except some improvements added later. The detailed expressions of the Gaunt factor in extremely relativistic bremsstrahlungs have been properly taken into account in Yamazaki et al. (2002), and the synchrotron emissivity for mildly relativistic cases (equation (23) in this paper) is also taken into account in this paper in addition to that for extremely relativistic cases (equation (21) in Kino et al. 2000).

In figure 2, curve *a* represents our best fit case, in which the curve fits very good not only to the X-ray luminosity and slope there but also to 4 points in IR and NIR range. The presence of inverted spectrum on the lower side of the synchrotron peak frequency clearly indicates that the radiation becomes opaque in this frequency region. Since the synchrotron emission becomes strong only where magnetic field is strong and temperature is high, it comes mainly from inner parts of the disk. The location of this inverted slope in the diagram is determined predominantly by the mass parameter m only. Therefore, we can

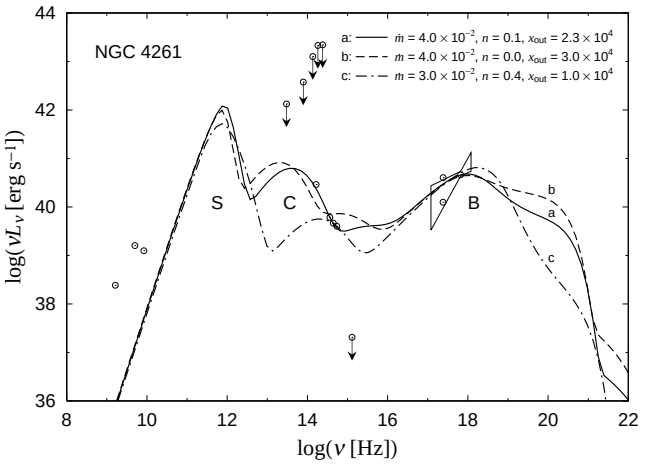

Fig. 2. Fittings to the observed spectrum of NGC 4261. The model curves are calculated based on our resistive RIAF model. The values of varied parameters are cited in the figure and those of fixed parameters are $m = 5$ and $\Re_0 = 10$ (or $\Delta = 6^\circ$).

say that the excess seen in the radio frequency range should be attributed to the components other than the accretion disk, most probably, to bipolar jet (Yuan 2007), unless the estimated black hole mass turns out to be larger by a few orders of magnitude.

A plateau like peak B is caused by thermal bremsstrahlung process, for which the low frequency side comes from outer parts of the accretion disk while the higher side comes from its innermost part. Peak C on the right hand side of peak S is due to the synchrotron photons once up-scattered by relativistic thermal electrons near the inner edge. We can also see on the higher side of C a slight peak caused by twice up-scattered photons. Such a peak is more evident on curve *b*. The effects of further multiple scatterings are neglected. Similarly to the case of synchrotron photons, the effects of inverse Compton scattering on the bremsstrahlung photons can be recognized in the frequency region above $\nu \sim 10^{21}$ Hz.

Beside our best-fit curve *a*, we show other curves *b* and *c* for comparison. Although the latter two curves also show good fits to the X-ray data, they have only poorer fits than the former in the IR range. Indeed, both curves do not go through the NIR point, and further, curve *b* goes through only one IR point out of three. Since curve *b* is a restricted fit within no wind condition ($n = 0$), the results strongly suggests that the presence of a disk wind in this object even if it may be week ($n \simeq 0.1$). Curve *c* is also a restricted fitting in which the outer edge radius is arbitrarily fixed at $x_{\rm out} = 10^4$. Although the difference in the values of $x_{\rm out}$ from the best-fit case is only a factor of 2, we need an extremely strong wind ($n = 0.4$) in this case. This may imply that the disk's outer edge radius can be determined fairly well by this kind of spectral fittings.

It is instructive to note the change in the shape of peak B according to an increase in the wind parameter n. As seen in the figure, it results in a decrease of the higher-frequency side shoulder of B. This is indeed an expected result, because as the disk wind becomes strong the matter that reaches deep down the accretion disk decreases and hence radiation produced there also decreases. Another point to mention is that for NGC 4261 we cannot find any explicit indication of a cool disk, which may be seen as an enhancement of the data points in ultraviolet (UV) range.

Thus, we have shown above that the radiation from a resistive RIAF disk can explain the main features of the observed spectrum of NGC 4261, and the parameters adopted in the previous section are very plausible ones.

5.2. Resistive RIAF as an absorber

Since a resistive RIAF is in LTE, a portion of good emitter is also a good absorber of the same radiation field. When it is placed in front of the counterjet, the jet emission is absorbed effectively by the part of the disk which can produce the corresponding emission. Therefore, the problem here is what part of the RIAF disk can contribute to the emission at 8.4 GHz. Since the synchrotron process is the dominant mechanism to produce this radio emission in a resistive RIAF, it works effectively in the place where both temperature and magnetic field are large. This corresponds to the innermost part of the disk. In order to evaluate the most efficient part of the accretion disk to produce the 8.4 GHz radio emission, specifically, we show in figure 3 different contributions to the total SED from several different partial disks. The dashed curves represent from the top the contributions from the disks whose inner edges are artificially truncated at $2r_{\rm in}$, $5r_{\rm in}$, $6r_{\rm in}$, $7r_{\rm in}$, $10r_{\rm in}$, respectively, while the full curve does the original SED.

Therefore the difference, for example, between the uppermost curve (the full curve) and the second curve (the uppermost dashed curve) represents the emission produced in the annular part of the disk with its radius in between $r_{\rm in}$ and $2r_{\rm in}$. It is evident from this figure that this innermost part of the disk contributes to the highest frequency parts of the synchrotron and bremsstrahlung emissions. The part which contributes mainly to 8.4GHz turns out from this figure to be the annulus between $6r_{\rm in}$ and $10r_{\rm in}$. Therefore, this part also acts most effectively in absorbing the radio of this frequency. Since the best fit parameters of the model SED indicate that the inner edge radius is $x_{\rm in} = 2.3\times10^2$, the absorbing annulus corresponds to $1.4\times10^3 r_{\rm S} < r < 2.3\times10^3 r_{\rm S}$. This size seems to be consistent with the observed distance from the core to the absorption gap (a few $\times10^3 r_{\rm S}$, see Jones et al. 2001).

If we define the spectral index of radiation as $\beta \equiv d\ln F_\nu / d\ln\nu$, it is related to the slope of the SEDs adopted in the present paper as $d\ln\{\nu F_\nu\}/d\ln\nu = 1+\beta \equiv \gamma$. The part of the disk which produces the radiation of a positive spectral index ($\beta > 0$ or $\gamma > 1$) is optically thick at that frequency and emitted radiation is self-absorbed. Therefore, we can read from figure 3 that the innermost part of the disk ($r_{\rm in} < r < 7r_{\rm in}$) is evidently opaque to the radiation near 8.4 GHz although its contribution to the radiation spectrum at these frequencies is rather small.

Figure 9 of Jones et al. (2001) show that the spectral index of the counterjet emission becomes very large (probably, $\beta > 2.5$) near the peak absorption, suggesting that it exceeds the value of self-absorbed synchrotron emission. Similar steep indices are observed also at the inner edge of the jet emission in NGC 1052 and interpreted as due to the free-free absorption

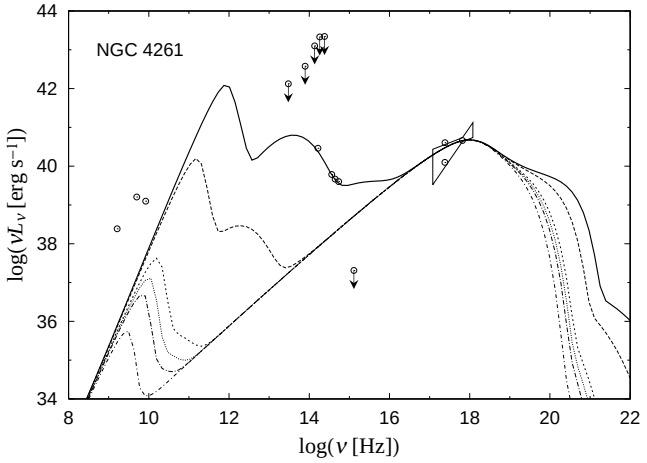

Fig. 3. Contributions to SED from different partial disks whose inner edges are artificially truncated at several radii. The full curve show the original SED which is the best fit case in figure 2, whose inner edge radius is written as $r_{\rm in}$. The dotted curves correspond from above to the truncations at $2r_{\rm in}$, $5r_{\rm in}$, $6r_{\rm in}$, $7r_{\rm in}$ and $10r_{\rm in}$, respectively.

by a circumnuclear torus (e.g., Kameno et al. 2005; Sawada-Satoh et al. 2008). Although these authors insist that such a steep index favors the interpretation in terms of free-free absorption by a foreground plasma, the same logic as theirs also apply to synchrotron absorption. It is a result of selective absorption of lower frequency parts caused by obscuring matter.

Owing to such a process, the incoming intensity $I_{\rm in}(\nu)$ attenuates like $I_{\rm in}\exp\{-\tau(\nu)\}$. Here $\tau(\nu)$ is the optical depth across the absorber, which is written as $\tau^{\rm sy}(\nu) \simeq (1/2)\alpha_\nu^{\rm sy} L$ in our case. As seen from equation (24), the frequency dependence of the synchrotron absorption coefficient is

$$\alpha_\nu^{\rm sy} \propto \nu^{-1}\exp(-\tau_0\nu^{1/3}) \tag{30}$$

with τ_0 being a constant, since $x_{\rm M} \propto \nu$. Thus, the attenuation becomes rapidly small as the frequency increases.

6. Summary and Conclusion

First, we have examined the plausibility of the assertion that the very narrow gap observed at radio frequencies in the counterjet emission of NGC 4261 is caused by the free-free absorption of a radiatively cooled accretion disk around its central black hole.

If the radiatively cooled disk is assumed to be optically thin, then the self-consistent model (SLE model) predicts that such a disk cannot be persistent, since it is known to be thermally unstable. In addition, such a disk is not geometrically thin and the optical depth is extremely small. Both these facts are unfavorable to explain the observations. On the other hand, if the disk is assumed to be an optically thick disk of the standard type, then the optical depth becomes too large and, further, the temperature in the disk turns out to be too small to maintain a sufficient ionization state, except in the region very close to the center.

Therefore, we may conclude that the emission gap is very unlikely to be caused by the free-free absorption of a radiatively cooled accretion disk of any type. Also, the low temperatures derived from the standard disk model strongly suggests the implausibility of realizing such disks, at least, in the outer accretion regions of NGC 4261 specifically, and also of similar type radio galaxies and of LLAGNs in general, all of which are accreting with very small fraction of each Eddington rate.

Next, we have examined the possibility of explaining the emission gap by a RIAF in a global magnetic field (i.e., resistive RIAF), and found that the model can actually explain both the appearance of the gap and the distance of peak absorption from the core, in terms of the synchrotron absorption caused by an inner part of the accretion disk. The model can also reproduce the observed global SED very well, except in the radio frequency range where the contribution from the jet is expected to be large.

Thus, we may conclude that the standard-type accretion disks, at least in its original form, do not exist anywhere in LERGs and nearby LLAGNs. Instead, the state of accretion flows in such objects are very likely to be described by the resistive RIAF model.

The resistive RIAF model predicts that a hot RIAF state is directly connected to a surrounding hot gas phase at around the Bondi radius from the center. In the case of NGC 4261, this radius is estimated to be $\sim 2.3\times10^4 r_{\rm S}$ from our spectral fittings, and is somewhat smaller than the inner radius of the geometrically-thin H I disk found by VLBI observations (van Langevelde et al. 2000). Although the H I disk seems to be connected to the outer HST dust torus (Jaffe et al. 1993), its relation to the accretion disks discussed in the present paper is still unclear.

The presence of such a circumnuclear tours is inferred also in NGC 1052 from radio observations (Kameno et al. 2005; Sawada-Satoh et al. 2008), and is expected to supply matter to the accretion disk enclosed within it. The central depression of the jet emission in this object and the steepening of its spectrum are interpreted as due to free-free absorption by this torus.

The resistive RIAF model also predicts that such an RIAF state cannot extends down to the last stable orbit around the central black hole, but terminates at the inner edge located at about $100\ r_{\rm S}$, where the effective magnetic Reynolds number becomes unity. Within this radius, the disk would become optically thick to synchrotron absorption up to $\sim 10^{12}$ Hz and expected to cool down to a temperature much lower than the virial one. Such a cool inner disk may resemble the standard disk, but, as already pointed out by some authors (e.g., Kuncic & Bicknell 2007), its radiation spectrum would be largely modified on account of the energy extraction caused by fairly strong vertical magnetic fields concentrated in this inner region. The detailed understanding of such processes, however, belongs to an attractive future work.

We would like to thank Seiji Kameno, the referee of this paper, for his several comments which were very useful to improve the manuscript. This work is partly supported by the Gant-in Aid for Scientific Research (C; 20540233, K. W.) from the Japanese Ministry of Education, Culture Sports, Science and Technology (MEXT).

References

Armitage, P.J. 2004, Ap&SS, 308, 89 (astro-ph/0405170)

Baganoff, F.K., Maeda, Y., Morris, M., Bautz, M.W., Brandt, W.N., Cui, W., Doty, J.P., Feigelson, E.D., Garmire, G.P., Pravdo, S.H., Ricker, G.R., & Townsley, L.K. 2003, ApJ, 591, 891

Ballantyne, D.R., Ross, R.R., & Fabian, A.C. 2002, MNRAS, 332, L45

Ballantyne, D.R., & Fabian, A.C. 2005, ApJL, 622, 97

Balmaverde, B., Capetti, A., & Grandi, P. 2006, A&A, 451, 35

Begelman, M.C., Sikora, M., & Rees, M.J. 1987, ApJ, 313, 689

Best, P.N., Kauffmann, G., Heckman, T.M., Brinchmann, J., Charlot, S., Ivezic, Z., & White, S.D.M. 2005, MNRAS, 362, 25

Cao, X. 2004, ApJ, 613, 716

Chiaberge, M., Capetti, A., & Celloti, A. 1999, A&A, 349, 77

Chiaberge, M., Capetti, A., & Celloti, A. 2000, A&A, 355, 873

Esin, A.A., McClintock, J.E., & Narayan, R. 1997, ApJ, 489, 865

Evans, D.A. Hardcastle, M.J., & Croston, J.H. 2007, in Extragalactic Jets: Theory and Observation from Radio to Gamma Ray, eds. Rector, T.A., & De Young, J.H., ASP Conf. Ser. 386, 161 (astro-ph/0707.2154v2)

Fabian, A.C., & Rees, M.J. 1995, MNRAS, 277, L55

Ferrarese, L., Ford, H.C. & Jaffe, W. 1996, ApJ, 470, 444

Frank, J., King, A., & Raine, D. 2002, Accretion Power in Astrophysics (Cmbridge University Press, Cambridge, UK) 3rd ed.

Gaskell, C.M. 2008, Rev Mexican A&A, 32, 1 (astro-ph/0711.2113v1)

Haardt, F., & Maraschi, L. 1991, ApJ, 380, L51

Hardcastle, M.J., Evans, D.A. & Croston, J.H. 2007, MNRAS, 376, 1849

Ho, L.C. 1999, ApJ, 516, 672

Ho, L.C. 2008, (astro-ph/0803.2268)

Jaffe, W., Ford, H.C., Ferrarese, L. van den Bosch, F. & O'Connell, R.W. 1993, Nature, 364, 213

Jones, D.L., Wehrle, A.E., Meier, D.L. & Piner, B.G. 2000, ApJ, 534, 165

Jones, D.L., Wehrle, A.E., Piner, B.G. & Meier, D.L. 2001, ApJ, 553, 968

Kaburaki, O. 2000, ApJ, 531, 210

Kaburaki, O. 2001, ApJ, 563, 505

Kaburaki, O. 2007, ApJ, 662, 102

Kaburaki, O. 2009, PASJ, 61, 429

Kameno, S., Nakai, N., Sawada-Satoh, S., Sato, N., & Haba, A. 2005, ApJ, 620, 145

Kato, S., Fukue, J., & Mineshige, S. 1998, Black-Hole Accretion Disks: Towards a New Paradigm (Kyoto University Press, Kyoto)

Kino, M., Kaburaki, O., & Yamazaki, N. 2000, ApJ, 536, 788

Kuncic, Z., & Bicknell, G.V. 2004, ApJ, 616, 669

Kuncic, Z., & Bicknell, G.V. 2007, Mod. Phys. Lett. A, 22, 1685

Leahy, J.P. 1999, in Astrophysical Disks, eds. Sellwood J.A., & Goodman, J. ASP Conf. Ser. 160, 246

Liu, S., Fromerth, M.J., & Melia, F. 2003, ApJ, 596, 879

Livio, M., Pringle, J.E., & King, A.R. 2003, ApJ, 593, 184

Mahadevan, R., Narayan, R., & Yi, I. 1996, ApJ, 465, 327

Maoz, D. 2007, MNRAS, 377, 1696

Merloni, A., & Fabian, A.C. 2002, MNRAS, 332, 165

Miller, J.M., Homan, J., & Miniutti, G. 2006, ApJ, 652, L113

Nandra, K., O'Neill, P.M., George, I.M., Reeves, J.N., & Turner, T.J. 2006, Astrn. Nachr., 327, 1039

Narayan, R. 2002, in Lighthouses of the Universe, eds. Gilfanov, M., Sunyaev, R., & Churazov, E., Springer, Berlin, 405

Narayan, R., Mahadevan, R., & Quataert, E. 1998, in Theory of Black Hole Accretion Disks, eds. M.A. Abramowicz, G. Bjornsson, J.E. Pringle (Cambridge University Press, Cabridge, UK) p148

Pringle, J.E., Rees, M.J., & Pachlczyk, A.G. 1973, A&A, 29, 179

Rees, M.J, Begelman, M.C., Blandford, R.D. & Phinny, E.S. 1982, Nature, 295, 17

Rybicki, G.B., & Lightman, A.P. 1979, Radiation Processes in Astrophysics (John Wiley & Sons, New York)

Rykoff, E.S., Miller, J.M., Steeghs, D., & Torres, M.A.P. 2007, ApJ, 666, 1129

Sawada-Satoh, S., Kameno, S., Nakamura, K., Namikawa, D., Shibata, M. K., & Inoue M. 2008, ApJ, 680, 191

Shakura, N.I., & Sunyaev, R.A. 1973, A&A, 24, 337

Shapiro, S.L., Lightman, A.P., & Eardley, D.M. 1976, ApJ, 204, 187

Sudou, H., Tanigich, Y., Ohyama, Y., Kameno, S., Sawada-Satoh, S., Inoue, M., Kaburaki, O., & Sasao, T. 2000, PASJ, 52, 989

Svensson, R., & Zdziarski, A.A. 1994, ApJ, 436, 599

Urry C.M., & Padovani P. 1995, PASP, 107, 803

van Langevelde H.J., Pihlstrom Y.M., Conway J.E., Jaffe W., & Schilizzi R.T. 2000, A&Ap, 354, L45

Yamazaki N., Kaburaki O., & Kino M. 2002, MNRAS, 337, 1357

Yuan F. 2007, in The Central Engine of Active Galactic Nuclei, eds. Ho L.C., & Wang J.-M., ASP Conf. Ser., 373, 95